International Journal of GEOMATE, Aug. 2023, Vol. 25, Issue 108, pp.138-145
ISSN: 2186-2982 (P), 2186-2990 (O), Japan, DOI: https://doi.org/10.21660/2023.108.3734
Geotechnique, Construction Materials and Environment

NUMERICAL ASSESSMENT OF SUBSEA PIPELINE PRESSURE CAPACITY DUE TO EXTERNAL CIRCUMFERENTIAL SEMI-ELLIPTICAL CRACK

Jason Filius Santoso[1], *Ricky Lukman Tawekal[1,2], Arianta[3], and Eko Charnius Ilman[1,2]

[1]Ocean Engineering Program, Institut Teknologi Bandung, Indonesia;
[2]Offshore Engineering Research Group, Institut Teknologi Bandung, Indonesia;
[3]Civil Engineering Program, Universitas Pertamina, Indonesia

*Corresponding Author, Received: 10 Dec. 2022, Revised: 19 Feb. 2023, Accepted: 19 April 2023

ABSTRACT: Crack defects in subsea pipelines may lead to pipe wall failure due to leak or rupture. Hence, crack analysis is essential to ensure pipeline integrity by assessing whether it is still fit for service. Cracks are evaluated using stress intensity factor (SIF) under certain loads by ensuring that this factor does not exceed the pipe material fracture toughness, at which point the crack initiates and propagates, leading to pipeline failure. A parametric study is performed to compute SIF values of circumferential semi-elliptical cracks on the external surface of a pipeline with a combination of crack depths of 4, 5, and 6 mm, and crack lengths of 20, 40, and 60 mm. An API 5L X65 grade pipeline with 254 mm outside diameter and 12.7 mm wall thickness is assessed by utilizing the extended finite element method. The models have been validated using theoretical SIF values calculated using API 579-1, with an average absolute deviation of 2.08%. It is concluded that for these cases, each millimeter increase in initial crack depth may reduce the pipeline pressure capacity up to 12 times compared to the initial crack length.

Keywords: Pipeline integrity, Stress intensity factor, Fracture mechanics, Semi-elliptical crack, XFEM

1. INTRODUCTION

Subsea pipeline remains to be the preferred solution for economically transferring hydrocarbon products between offshore facilities or towards land facilities for export. It is a considerably safe and competitive option compared to FPSO and tankers for up to 1500 km in distance with up to 50 years of service life [1]. Nevertheless, pipelines designed under strict standards and safety requirements are still susceptible to damage. Mechanical damages on pipelines due to fabrication flaws or operational damages often manifest themselves as cracks [2].

Cracks are flaws on a body, with a characteristic depth and length as well as a sharp angle at the root [3]. These may appear in numerous variations of size, position, and geometry, but some general idealized forms include surface, embedded, and through-wall cracks. Cracks may appear on a pipeline due to lack of welding fusion or penetration during fabrication, sharply localized corrosion during service, a combination of corrosion, residual stress, and poor microstructure of steel, or even third party impacts such as anchoring or vessel collision [4]-[8].

Most pipeline systems are under cyclic loads such as currents, waves, or seabed movements during its operational period [9]. These fluctuating loads may cause fractures such as cracks to initiate and propagate [10], causing fatal failure of the pipe. It is essential to prevent a crack from propagating which may lead to pipe leakage or burst. Preventive measures taken to avoid crack propagation is preventing the crack from initiating in the first place. This is a more reasonable approach compared to inventing a new material strong enough to withhold propagation. The crack initiation process itself does not involve propagation, however it is regarded as a permanent deterioration of material strength [11].

Once a crack is identified on an operating pipeline, the conventional ratio of operational stress to the yield strength of the pipe cannot be the only integrity acceptance criterion, but fracture mechanics needs to be taken into consideration [12]. A common measure in crack analysis is the stress intensity factor (SIF), which predicts the state of stress in a point near the crack tip on an elastic material under a specified load [3]. The crack and structure geometry, together with the applied loads, influence the value of SIF. The crack tip initiates once its SIF value exceeds the pipe fracture toughness which is a measure of material ability to resist crack initiation and propagation.

The value of SIF of an existing crack can be obtained by numerical modeling of the crack on a pipe using the extended finite element method (XFEM). This paper studies a specific case of initial crack on a pipeline with the aim of obtaining its SIF value, which is then validated using a theoretical value. A parametric study is performed to assess SIF values of nine cases of circumferential semi-elliptical cracks on the external surface of an X65 pipeline with a combination of crack depths of 4, 5, and 6 mm, and crack lengths of 20, 40, and 60 mm. The validated models are then analyzed to further assess the maximum pressure capacity to avoid crack propagation.

2. RESEARCH SIGNIFICANCE

Using the extended finite element method, this study presents a relatively straightforward validated numerical model for calculating the SIF value of a specific pipeline crack geometry. The proposed method reduces the complexity of the model configuration and mesh structuring, so it can be used to conduct a preliminary assessment of the remaining pressure capacity of a cracked pipeline in a short amount of time, which is advantageous to ensure that the pipeline is still fit for service. Using the same methods described in this study, other crack dimensions can be evaluated.

3. STRESS INTENSITY FACTOR OF A SEMI-ELLIPTICAL EXTERNAL SURFACE CRACK (CIRCUMFERENTIAL DIRECTION)

Stress intensity factor determines the stress state of an elastic material near a crack tip. This paper specifically studies one case of crack geometry which is an external circumferential semi-elliptical crack with axial loading, as illustrated in Fig. 1. API 579-1 provides an extensive compendium of stress intensity factor solutions to numerous cases of crack geometry, structure geometry, and loading configuration, with a wide range of crack dimension applicability. Therefore, the formula to calculate theoretical SIF value of the crack as shown in Eq. (1) is obtained from [3] as follows:

$$K_{\mathrm{I}} = G_0\left(\frac{pR_{\mathrm{i}}^{\,2}}{R_{\mathrm{o}}^{\,2}-R_{\mathrm{i}}^{\,2}}+\frac{F}{\pi\left(R_{\mathrm{o}}^{\,2}-R_{\mathrm{i}}^{\,2}\right)}\right)\sqrt{\frac{\pi a}{Q}} \qquad (1)$$

where stress intensity factor is represented by K_I, G_0 is the geometry factor, p is the internal pressure of pipe, inner and outer pipe radius are represented by R_{i} and R_{o} respectively, F is the applied axial force on pipe, the crack depth is a, and Q is a parameter calculated with the following expression:

$$Q = \begin{cases} 1.0 + 1.464\left(\dfrac{a}{c}\right)^{1.65} & \text{for } a/c \le 1.0 \\ 1.0 + 1.464\left(\dfrac{c}{a}\right)^{1.65} & \text{for } a/c > 1.0 \end{cases} \qquad (2)$$

where c is half of the crack length.

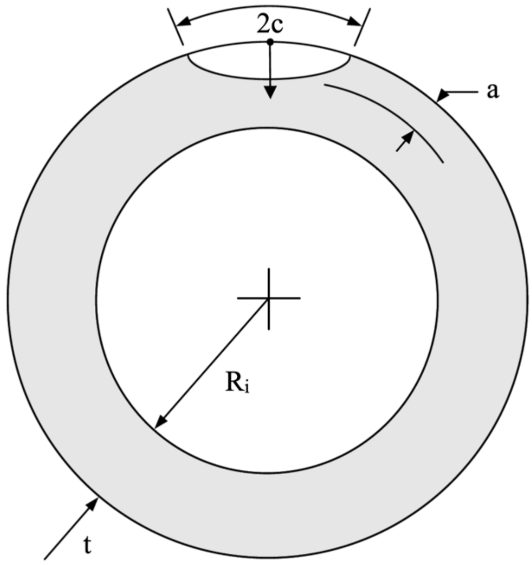

Fig. 1 External circumferential semi-elliptical crack on a cylinder, showing the defined *a* and *2c* parameters [3]

4. EXTENDED FINITE ELEMENT METHOD

Conventional finite element modeling is widely used to obtain approximate solution to differential equations in numerical models. However, this method becomes relatively complex and inefficient in modeling discontinuities due to the high computational power required to reach solution convergence [13]. This limitation is due to the need of a detailed mesh that follows the crack geometry and constant remeshing in modeling crack growth.

Belytschko and Black [14] offered a solution to the finite element method limitation by developing extended finite element method (XFEM). XFEM is capable of analyzing models with discontinuities while eliminating complex mesh requirements [15].

4.1 XFEM Solution Equation

The displacement solution given by XFEM adopts partition of unity as its framework, where a jump function and a near-tip asymptotic function are used to enrich finite elements affected by a crack [2]. Fig. 2 illustrates this concept.

The approximate displacement vector solution is expressed as follows [16]:

$$\mathrm{u} = \sum_{i=1}^{\mathcal{N}} N_i(x)\left[u_i + H(x)a_i + \sum_{j=1}^{4}\psi_j(x)b_i^j\right] \qquad (3)$$

where u is the displacement vector, shape function is represented as $N_i(x)$, u_i represents the elements unaffected by crack degree of freedom (DoF) vector, heaviside jump function is $H(x)$, a_i is the split elements DoF vector, $\psi_j(x)$ is the asymptotic crack tip function, and b_i^j is the DoF vector of elements containing a crack tip.

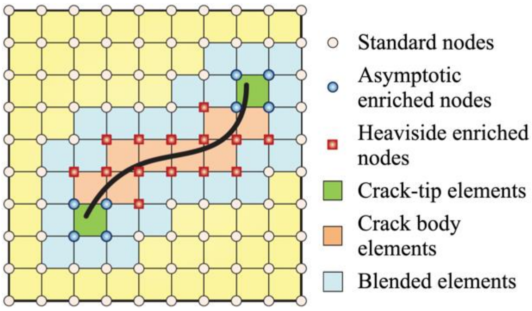

Fig. 2 Typical crack modeling with XFEM [13]

4.2 XFEM Model for SIF Evaluation

XFEM can be used to evaluate contour integrals and SIF along the crack tip without an overly detailed and refined mesh [15]. However, the mesh structure should not be constructed arbitrarily. This study adopts a recommended guideline to XFEM meshing for SIF computation provided in [16] such as the element depth of the crack region mesh should be less than 13% of crack depth (a) and the number of contours for SIF calculation is at least 7. SIF is calculated in each contour involved, which are element rings surrounding a crack tip, illustrated in Fig. 3. The target accuracy of this method is less than 10% deviation from the theoretical SIF value.

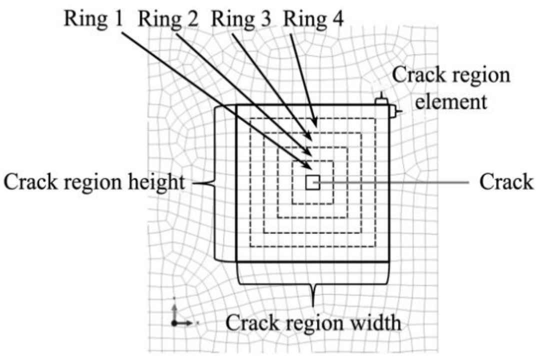

Fig. 3 Five contours around a crack tip [16]

5. NUMERICAL MODELING

Abaqus FEA is utilized in this study to perform XFEM modeling. A pipe with the crack model is constructed to perform Abaqus SIF calculation. This model will then be validated by comparing the Abaqus SIF with the theoretical SIF using Eq. (1).

5.1 General Pipe Model and Crack Cases

In this study, the pipe specimen is modeled based on a case study in [17], which is an existing pipeline system in Madura Strait, Indonesia. Table 1 shows relevant design parameters of the pipeline system.

The pipe is modeled in Abaqus as a solid part with a length of 120 mm, while the crack is modeled as a planar shell part with several different dimensions of depth and length, as shown in Table 2. Fig. 4 dan Fig. 5 show an example visualization of the general model.

Table 1 Pipeline design parameters [17]

Parameter	Unit	Value
Material	API 5L X65 PSL2	
Outer Diameter	mm	254
Wall Thickness	mm	12.7
Young's Modulus	GPa	207
SMYS	MPa	490
SMTS	MPa	507
Operating Pressure	MPa	12.962
Fracture Toughness	$\text{MPa}\sqrt{\text{m}}$	168.907

Note: Fracture Toughness is calculated in [17] using equations from [3]; SMYS = Specified Minimum Yield Strength; SMTS = Specified Minimum Tensile Strength

Table 2 Studied crack dimensions

Case	Crack Depth (a)	Crack Length ($2c$)
1	4 mm	20 mm
2	4 mm	40 mm
3	4 mm	60 mm
4	5 mm	20 mm
5	5 mm	40 mm
6	5 mm	60 mm
7	6 mm	20 mm
8	6 mm	40 mm
9	6 mm	60 mm

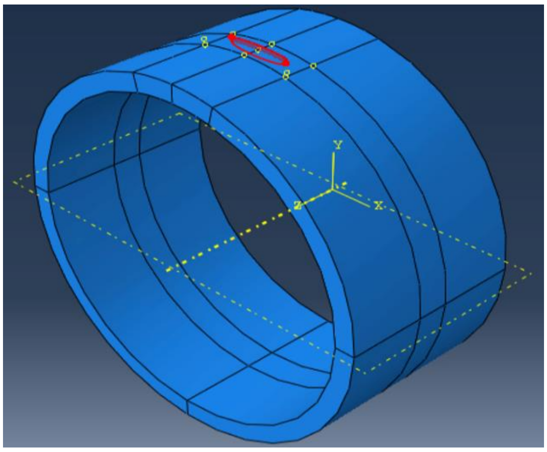

Fig. 4 Pipe model in Case 5

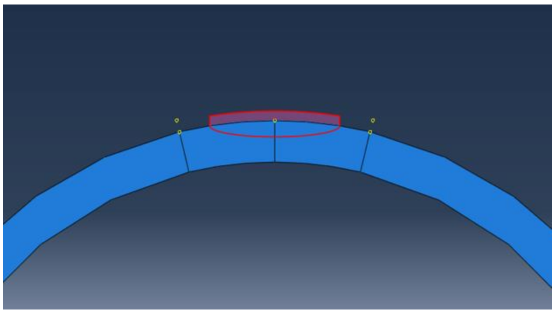

Fig. 5 Crack model in Case 5

5.2 Mesh Configuration

For each studied crack case, a compatible mesh configuration is constructed. This is done by applying the guidelines from [16] as previously described. However, it is important to note that more refined mesh will require higher computational power. In this model problem, the maximum allowable number of elements involved in the calculation is roughly 180000 based on the available computational resource. With the existing constraints, limitations, and the provided guidelines, a crack region mesh is constructed in a way that can accommodate at least 7 element contours with the largest element size allowed.

In the crack region, the depth of each element (h_y) is set to be 13% of the crack depth. The size of other two sides of the element (h_x and h_z) is taken as around 2 times the depth (h_y). This will result in a rectangular prism shaped element. Each element can be set as a cube for better accuracy, but this will result in a significantly higher number of elements involved.

A mesh convergence study is performed for Case 1 as a reference to compare the computation accuracy based on the number of contours used. According to [16], the minimum number of contours needed for SIF evaluation is 7. It is attempted to compute SIF with a coarser mesh of 5 and 6 contours using the same method of mesh construction. The number of contours is directly proportional to the total number of elements.

It is concluded from Fig. 6 that using more contours results in higher accuracy of SIF computation. However, all SIF deviations from the theoretical value are still under the maximum allowable deviation of 10%, therefore all results in Fig. 6 are still acceptable based on [16]. Nevertheless, SIF computation with at least 7 contours still bears the most accurate result. This reverifies the guidelines given in [16] and no further mesh study is done due to the computation capacity limitations mentioned and enough accuracy has been achieved for SIF evaluation in this study.

An example crack region configuration for one crack case can be seen in Fig. 7. The crack region dimensions (L_x and L_z) are approximated to accommodate at least 7 contours around the surface crack tips based on h_x and h_z, as shown in Fig. 8. For better accuracy, the crack tips on the surface should be located in the middle of a certain element, not coinciding with a node or element boundary. This also applies to the deepest crack tip, shown in Fig. 9. If these three particular tips are not positioned at the center of an element, the crack region element sizes h_x , h_y and h_z should be modified accordingly while maintaining at least 7 contours around the crack tips.

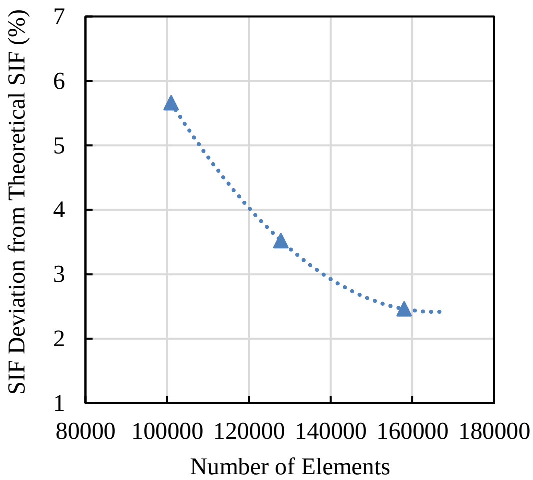

Fig. 6 Number of elements vs SIF deviation for Case 1

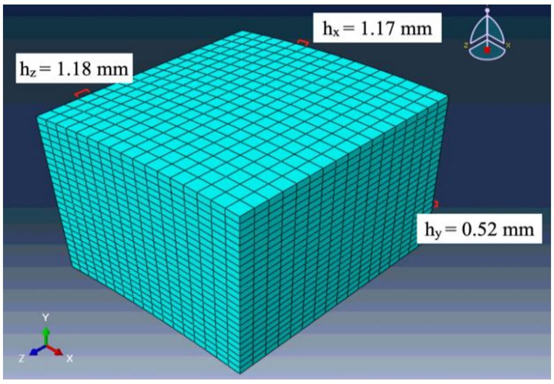

Fig. 7 Crack region mesh in Case 1

For the elements outside the crack region, it is taken 5 mm as the seed size. A smaller global element seed size can be used but with the cost of more computational power. Global element size is likely more flexible than in the crack region since there will be no SIF computation in that finite element field. These procedures are repeated for each studied crack to achieve the most suitable configuration for each case. Table 3 summarizes the mesh configurations for all 9 crack cases.

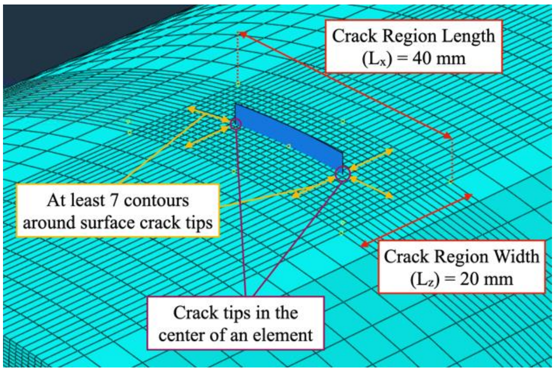

Fig. 8 Crack region in Case 1

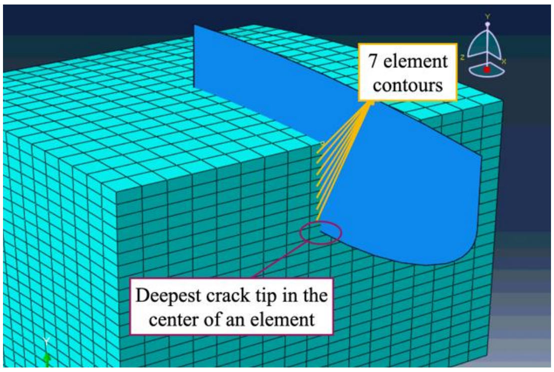

Fig. 9 Deepest crack tip in Case 1

Table 3 Crack dimensions and mesh configurations for all cases

Case	1	2	3	4	5	6	7	8	9
$\boldsymbol{a}$ (mm)	4	4	4	5	5	5	6	6	6
$\boldsymbol{2c}$ (mm)	20	40	60	20	40	60	20	40	60
$\boldsymbol{h_y}$ (mm)	0.52	0.52	0.52	0.65	0.65	0.65	0.72	0.72	0.72
$\boldsymbol{h_z}$ (mm)	1.18	1.18	1.18	1.33	1.33	1.33	0.84	0.84	0.84
$\boldsymbol{h_x}$ (mm)	1.17	1.23	1.21	1.32	1.28	1.29	0.79	0.82	0.82
$\boldsymbol{L_z}$ (mm)	20	20	20	20	20	20	16	16	16
$\boldsymbol{L_x}$ (mm)	40	60	80	40	60	80	40	60	80
Contours	7	7	7	7	7	7	8	8	8
Global mesh (mm)	5	5	5	5	5	5	5	5	5
Total Elements	158064	166944	177600	121800	130200	137200	136188	148824	161460

5.3 Loading and Boundary Condition

The applied loads in the pipe model consist of pipe internal pressure and longitudinal stress. According to Eq. (1), this case of SIF calculation considers only axial stresses on the pipe, which are the internal pressure converted to longitudinal stress and any axial forces converted to stress working on the pipe cross section. Therefore, if there are no presence of other external axial forces is taken as an assumption, the longitudinal stress modeled in Abaqus is only derived from the internal pressure using Eq. (4) as follows:

$$\sigma_{\mathrm{L}} = \frac{pR_{\mathrm{i}}^{2}}{R_{\mathrm{o}}^{2} - R_{\mathrm{i}}^{2}} \tag{4}$$

where σ_{L} is the longitudinal stress. Fig. 10 illustrates the concept of calculating longitudinal stress from internal pressure in a cylinder.

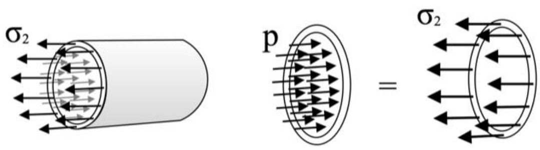

Fig. 10 Longitudinal stress in cylinder

Longitudinal stress is only applied on one side of the cylinder while the other side is given a symmetry boundary condition as shown in Fig. 11 and Fig. 12.

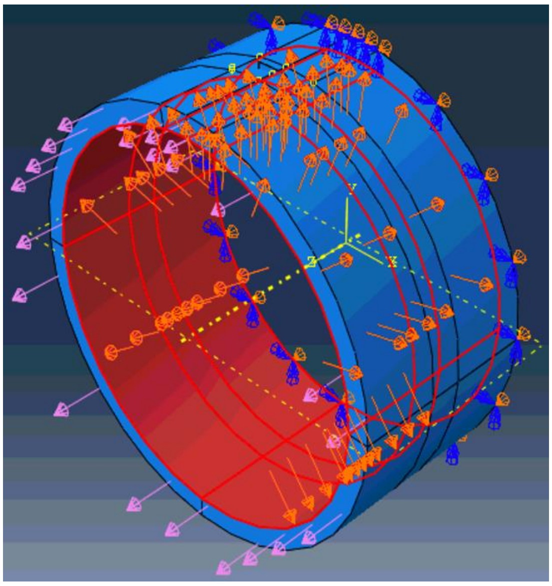

Fig. 11 Internal pressure load

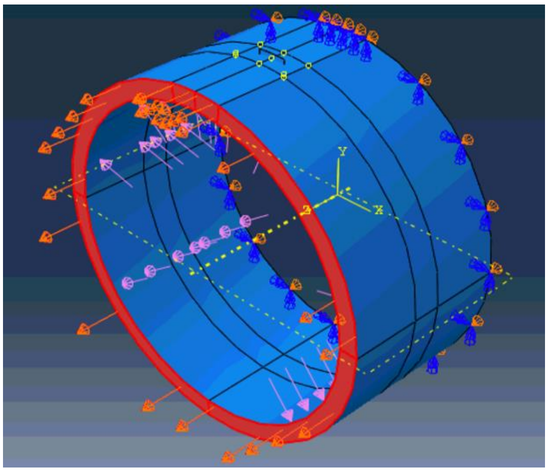

Fig. 12 Longitudinal stress load

6. RESULTS

The results of this study include the calculation of theoretical SIF value for each crack case using the formula given by [3], the results of SIF calculation with Abaqus XFEM modeling, and maximum internal pressure capacities for each crack case.

6.1 Theoretical SIF Values

Theoretical SIF calculation is done to obtain a reference to validate the crack model. In this study, only the deepest point of the crack will be observed, both in theoretical calculation and software modeling. Table 4 summarizes the value of theoretical SIF for each crack case which is determined at its respective deepest point on the pipe using Eq. (1).

It is clear that the SIF value for every case is way below the fracture toughness of the pipe material shown in Table 1. This indicates that the pipe is still fit for service under normal operational conditions and will not cause these cracks to propagate deeper into the pipe.

Table 4 Theoretical SIF values

Case	a (mm)	$2c$ (mm)	SIF (MPa$\sqrt{\text{m}}$)
1	4	20	6.433
2	4	40	7.760
3	4	60	8.356
4	5	20	6.784
5	5	40	8.691
6	5	60	9.759
7	6	20	7.120
8	6	40	9.692
9	6	60	11.177

6.2 XFEM-Computed SIF Values

Abaqus computes SIF in all the contours involved as set by the user. The average value of SIF throughout all the contours is taken as the Abaqus SIF. Table 5 contains the result of Abaqus SIF calculation for the deepest point of each crack.

Table 5 Theoretical and Abaqus SIF comparison

Case	Theoretical SIF (MPa$\sqrt{\text{m}}$)	Abaqus SIF (MPa$\sqrt{\text{m}}$)	Deviation
1	6.433	6.591	2.46%
2	7.760	7.731	-0.37%
3	8.356	8.305	-0.62%
4	6.784	6.915	1.94%
5	8.691	8.612	-0.91%
6	9.759	9.406	-3.61%
7	7.120	7.379	3.63%
8	9.692	9.543	-1.54%
9	11.177	10.770	-3.65%

Table 5 shows that all the SIF value obtained from Abaqus modeling deviate below 5% from its theoretical value with the maximum and minimum deviations of 3.65% and 0.37%, respectively. The average absolute deviation throughout all nine cases is 2.08%. The deviation values may seem inconsistent between cases. These differences are considered due to the variability and irregularity of crack dimensions and element shapes for each case. These factors then affect the accuracy of SIF numerical calculations along the crack path.

The deviations are considered acceptable since they are all below the recommended 10% maximum deviation given by [16]. This allows the XFEM models to be used for maximum pressure capacity calculations for the nine cases as described in sub section 6.3, or as validation materials for future complex crack assessment studies. These maximum pressure capacities are assessed to study the effects of initial crack depth and length.

6.3 Maximum Internal Pressure Capacities

From the modeling results, it is attempted to obtain internal pressure values that will potentially cause each crack case to initiate and propagate inwards, posing a pipe leakage threat. The approach taken in this study is iterative trial-and-error which is done by incrementally increasing the internal pressure and the consequent longitudinal stress loads until the SIF value is equal to the fracture toughness. Table 6 summarizes the maximum internal pressure capacity of a pipeline given that the pipeline possesses a certain initial crack.

Table 6 Maximum Internal Pressure Capacity for Respective Initial Crack Dimensions

Case	a (mm)	$2c$ (mm)	Operating SIF (MPa$\sqrt{\text{m}}$)	Maximum Internal Pressure Capacity (MPa)
1	4	20	6.591	332.193
2	4	40	7.731	283.176
3	4	60	8.305	263.669
4	5	20	6.915	316.592
5	5	40	8.612	254.213
6	5	60	9.406	232.761
7	6	20	7.379	296.716
8	6	40	9.543	229.439
9	6	60	10.770	203.299

Through iteration results it is obtained that each maximum pressure capacity applied to the cracked pipeline model causes the value of SIF at the deepest tip of the initial crack to reach the pipe fracture toughness with extremely small deviations (less than 0.005%). This signifies that these pressures can be taken as the values that will initiate an identified existing crack to propagate further deep into the pipe. These maximum pressure capacities are significantly higher than the designed operating pressure (12.962 MPa) due to the small dimensions of the studied crack cases, but it is clear that larger initial cracks, both in depth or length, lead to a lower maximum capacity the pipe can withstand before the crack initiates and propagates.

Fig. 13 and Fig. 14 are drawn to illustrate the influence of initial crack length and depth to the maximum pressure capacity of the pipe. The downward trend of this capacity as the initial crack dimensions increase becomes more apparent. Linear regressions are calculated for all cases of the same initial crack length with an increasing initial crack depth as in Fig. 13, and cases of the same initial crack depth with an increasing initial crack length as in Fig. 14. From these linear regressions, the gradient of each trendline is obtained and can be perceived as how influential a crack parameter is to the maximum pressure capacity. The average gradient of the three trendlines in Fig. 13 is -24.93 while the average in Fig. 14 is -2.05. This shows an indication that the effect of initial crack depth to the maximum capacity is much more prominent than the initial crack length. Each millimeter increase of the initial crack depth reduces the maximum capacity about 12 times more than each millimeter increase in initial crack length.

Realistically, at these extremely high internal pressures, the pipe material itself may have failed by yield failure mode even before the crack initiates since pipe systems are not necessarily designed to withstand pressures over ten times its intended operating pressure. It is also possible for the crack to not propagate deeper into the pipe, but sideways to the longitudinal direction due to the significantly high hoop stress from the internal pressure.

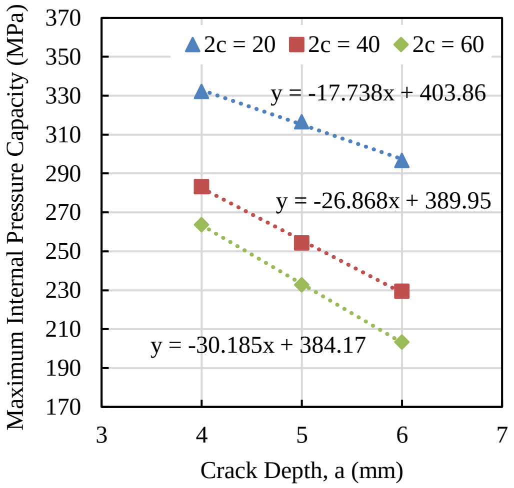

Fig. 13 Maximum Internal Pressure Capacity vs. Initial Crack Depth

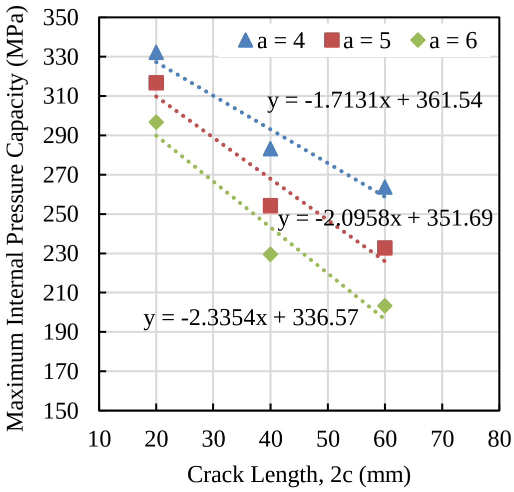

Fig. 14 Maximum Internal Pressure Capacity vs. Initial Crack Length

7. CONCLUSION

This study successfully assessed SIF values of nine variations of initial cracks on a subsea pipeline with a maximum deviation of 3.65% from its theoretical SIF value which is calculated using Eq. (1) from [3]. Extended finite element method on Abaqus is used to eliminate complex meshing configuration of the crack region such as that in conventional finite element method.

It is concluded that all cases of initial crack will not propagate deeper into the pipe based on Abaqus SIF evaluation. The largest variation of the studied crack dimensions yields an SIF value of only 10.77 MPa$\sqrt{\mathbf{m}}$ which is significantly lower than the pipe fracture toughness, 168.907 MPa$\sqrt{\mathbf{m}}$, therefore the pipe is still fit for service under normal operating conditions. Larger initial crack depth and length both result in higher SIF value, therefore the pressure at which the crack will initiate and propagate deeper into the pipe is lower. It is obtained that the smallest crack variation results in a maximum pressure capacity of 332.193 MPa, while the largest crack variation results in a 38.8% lower capacity of 203.299 MPa. In this particular case, initial crack depth is around 12 times more influential to the decrease of maximum pressure capacity compared to the initial crack length.

The construction of XFEM models in this study is conducted to provide a valid methodology of SIF calculation. Therefore, this methodology can be utilized to assess the SIF of complex crack geometries and loading configurations which are yet to have empirical SIF formulas. This XFEM modeling for complex cracks is suggested to be an alternative to evaluate SIF efficiently.

8. ACKNOWLEDGEMENTS

The authors gratefully acknowledge the financial support from Institut Teknologi Bandung for this work under research grants of Research, Community Service, and Innovation Program (P2MI), and software license from Civil Engineering Program, Universitas Pertamina.

9. REFERENCES

[1] Kenny, S., Offshore Pipelines—Elements of Managing Risk, Methods in Chemical Process Safety, Vol. 2, Cambridge, Eds. F. Khan, H. Pasman, and M. Yang, Academic Press, 2018, pp. 289-325.

[2] Shi, J., Chopp, D., Lua, J., Sukumar, N., and Belytschko, T, Abaqus implementation of extended finite element method using a level set representation for three-dimensional fatigue crack growth and life predictions, Engineering Fracture Mechanics, Vol. 77, Issue 14, 2010, pp. 2840-2863.

[3] American Petroleum Institute, Fitness-for-Service API 579-1, Washington, D.C., API Publishing Services, 2016, pp. 1-1320.

[4] Fearnehough, G. D., Fracture propagation control in gas pipelines: A survey of relevant studies, International Journal of Pressure Vessels and Piping, Vol. 2, Issue 4, 1974, pp. 257-282.

[5] Mohtadi-Bonab, M. A, Effects of Different Parameters on Initiation and Propagation of Stress Corrosion Cracks in Pipeline Steels: A Review, Metals, Vol. 9, Issue 5, Article 590, 2019, pp. 1-18.

[6] Tawekal, R. L., Allo, R. P. R., and Taufik, A., Damage Analysis of Subsea Pipeline Due to Anchor Drag, International Journal of Applied Engineering Research, Vol. 12, Issue 15, 2017, pp. 5016-5021.

[7] Tanujaya, V. A., Tawekal, R. L. T., and Ilman, E. C, Vessel traffic geometric probability approaches with AIS data in active shipping lane for subsea pipeline quantitative risk assessment against third-party impact, Ocean Systems Engineering, Vol. 12, Issue 3, 2022, pp. 267-284.

[8] Tawekal, R. L .T. and De Velas, J, Subsea Pipeline Protection Design Subjected to Dropped Anchor Using Concrete Mattress, International Journal of GEOMATE, Vol. 17, Issue 60, 2019, pp. 251-258.

[9] Zhang, Y., Xiao, Z., and Luo, J, Fatigue crack growth investigation on offshore pipelines with three-dimensional interacting cracks, Geoscience Frontiers, Vol. 9, Issue 6, 2017, pp. 1689-1697.

[10] Liu, H. B. and Zhao, X. L., Fatigue of Subsea Pipelines Under Combined Actions, in 23rd International Offshore and Polar Engineering Conference, 2013, pp. 147-154.

[11] Paredes, M., Wierzbicki, T., & Zelenak, P., Prediction of Crack Initiation and Propagation in X70 Pipeline Steels, Engineering Fracture Mechanics, Vol. 168, Issue A, 2016, pp. 92-111.

[12] Anderson, T. L., Fracture Mechanics Fundamentals and Applications, 4th ed., Boca Raton, CRC Press, 2017, pp. 1-680.

[13] Khoei, A. R., Extended Finite Element Method Theory and Applications, Chichester, Wiley & Sons, 2015, pp. 1-587.

[14] Belytschko, T. and Black, T., Elastic crack growth in finite elements with minimal remeshing, International Journal for Numerical Methods in Engineering, Vol. 45, Issue 5, 1999, pp. 601-620.

[15] Arianta, Tawekal, R. L., Taufik, A., and Rildova, Determination of Geometry Factor of Crack in Dented API 5L X65 Pipeline Using Finite Element Method, International Journal of Scientific & Engineering Research, Vol. 6, Issue 1, 2015, pp. 1343-1349.

[16] Levén, M. and Rickert, D., Stationary 3D Crack Analysis with Abaqus XFEM for Integrity Assessment of Subsea Equipment, Göteborg, Chalmers University of Technology, 2012, pp. 1-87.

[17] Qauli, S. F, Engineering Critical Assessment of Subsea Pipeline with S-Lay Installation Method, Bandung, Institut Teknologi Bandung, 2021, pp. 1-88. (in Bahasa Indonesia)